FOSREM®

# Fiber Optics System for Rotational Events&Phenomena Monitoring

Support under grant PBST1/83/ 7/2012

FOSREM

# Investigation of Building Rotational Motion Using Set of AFORSs (Autonomous Fibre Optic Rotational Seismographs)

L.R. Jaroszewicz*, Z. Krajewski*, M. Matysik*, J.K. Kowalski**

*Institute of Technical Physics, Military University of Technology

Gen. Sylwestra Kaliskiego Str. 2, 00-908 Warsaw, POLAND

**m-Soft Ltd., Sotta „Sokoła" Str. 9-4, 02-790 Warsaw, POLAND

FOSREM

# Outline

- Sagnac effect – how its use for rotation monitoring?
- Rotational Seismometer – why not FOG?
- Autonomous Fibre-Optic Rotational Seismographs:
  - optic and electronic part construction
  - calibration and accuracy estimation,
  - remote control
- AFORSs application for monitoring building rotation
- Outcome
- Conclusions

# Sagnac effect

1913 Georges Sagnac – interferometer for rotation detection where the two directions within the rotating loop see slightly different optical paths. Sagnac's original experiment used a loop about 1m square and detected fringes shift when the loop rotated at a few times a second.

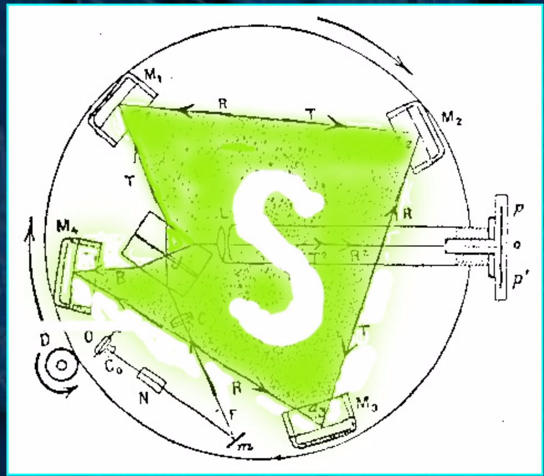

[Post, *Rev. Mod. Phys., 39, 1967*]

$$\Delta Z = 4 \frac{\Omega . S}{\lambda_0 c}$$

The Sagnac interferometer measures rotation with respect to the fixed star in the galaxy, rather than with respect to the rotating Earth's surface.

The observed fringe shift does not depend on:

- the presence of a comoving refracting medium in the path of the beam,
- the shape of surface area S,
- the location of the center of rotation.

# How is use for rotation monitoring?

$$\phi_S = \frac{2\pi L D}{\lambda c}\Omega$$

L=10 m, D=15 cm,

λ=630 nm

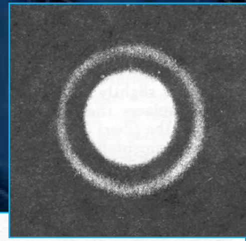

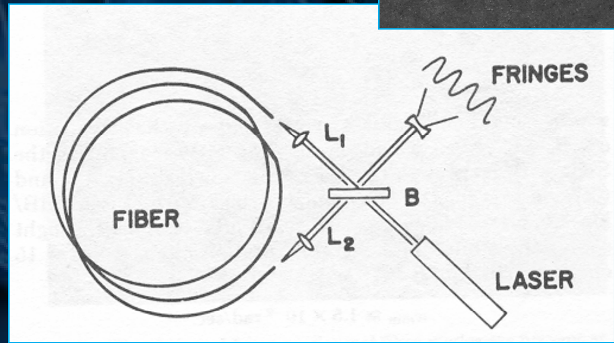


[Vali et al, *Appl. Opt., 15(5), 1976*]

The phase shift increase with L – practical way for FOG development.

The reciprocal condition for ϕ detection – the reciprocal configuration [Urlich, 1980] also called the minimum configuration [Arditty and LeFevre, 1981]

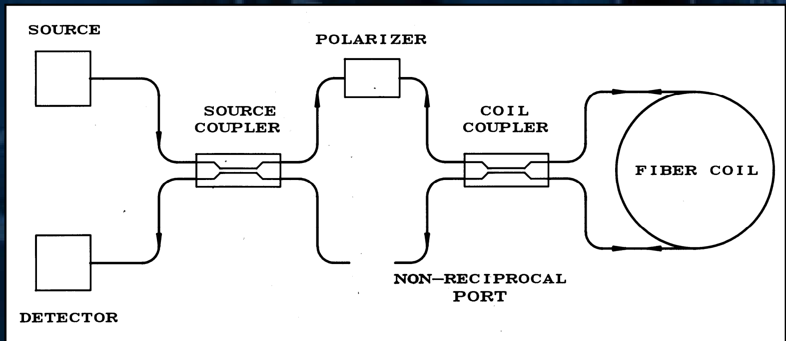


Combined single-spatial-mode and single-polarization filtering at the common input-output port

# Rotational Seismometer – why not FOG?


$$\Delta\phi = \frac{4\pi RL}{\lambda c}\Omega = \frac{1}{S_o}\Omega$$

Fibre-Optic Rotational Seismometer FORS optimization:

1. Optical Unit – increase sensitivity & minimalization external influences
2. Electronic Unit - proper signal processing for long time operation & remote control

$$FOG \Rightarrow \vartheta = \int \Omega\, dt$$

Problems with:

1. Drift phenomenon,
2. Dynamic range,
3. Applied dedicate electronics for angle not rotation speed detection,
4. …,

# Influence of SMF-28 fibre lenght on system sensitivity for constructed AFORS

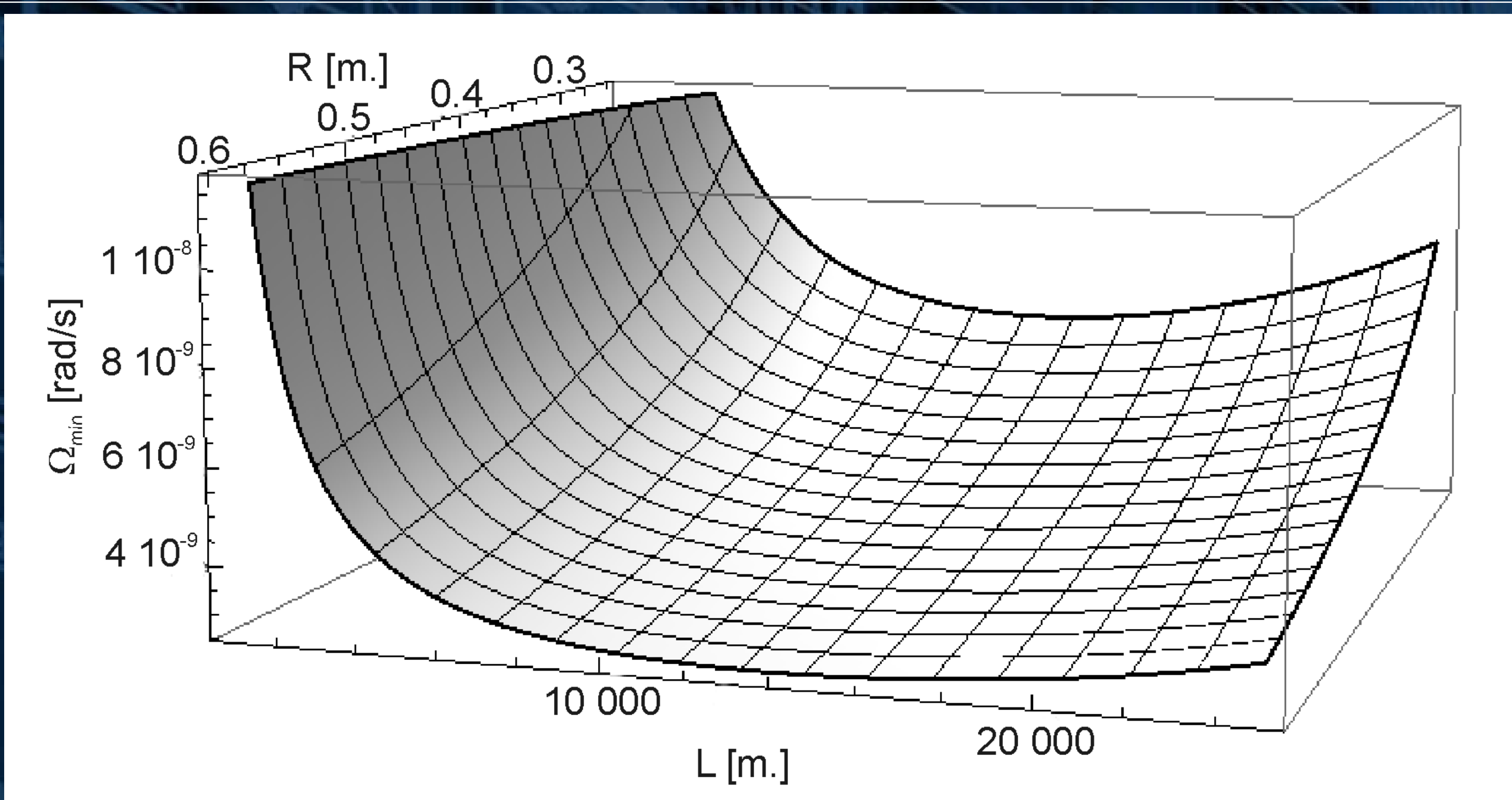


AFORS resolution versus total optical length *L* and loop radius in 1 Hz detection band. Parameters for simulation: wavelength $\lambda$=1285 nm, fibre attenuation $\alpha$= 0.45 dB/km, optical path loss $\sigma$=15 dB, optical power *P*= 20 mW [L. R. Jaroszewicz, et al., in R. Teisseyre, H. Nagahama, E. Majewski (eds.), *Physics of Asymmetric Continuum: Extreme and Fracture Processes*, Spinger-Verlag, Chap. 2, 2008.]

# Autonomous Fibre-Optic Rotational Seismographs

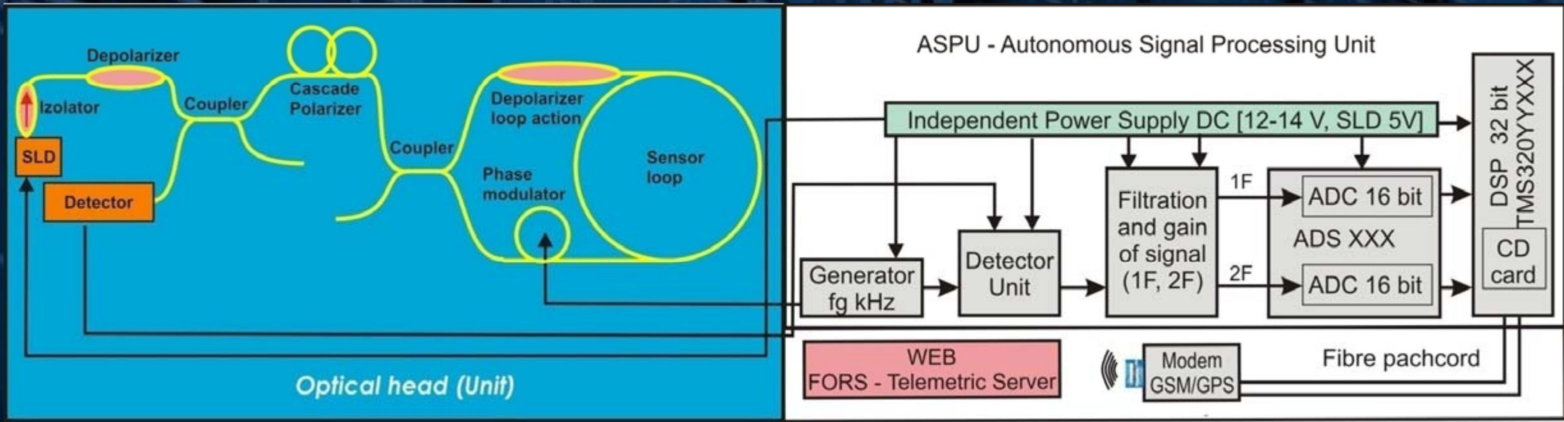


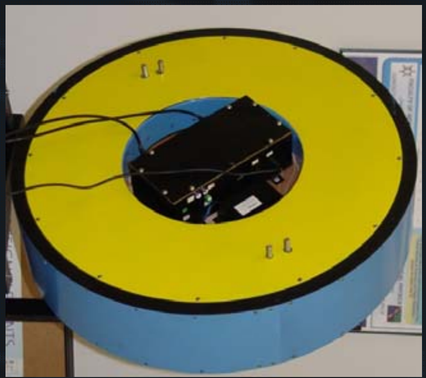

**AFORS-2**

**$\Omega_t$=2.46·10$^{-9}$ rad/s/Hz$^{1/2}$**

L= 15 000 [m], 15 layers, double quadropole winded, $\alpha$ =0.446 [dB/km], loop R=0.340 [m] contains permaloy particles, $\sigma$ = 13.16 [dB], cascade polarizers (46 and 55 [dB]), depolarizer with 0.02 [dB] extinction ratio, $\Delta\lambda$=31,2 [nm], $\lambda$=1326.9 [nm], $P_L$ =20 [mW], fg=6.8 kHz.

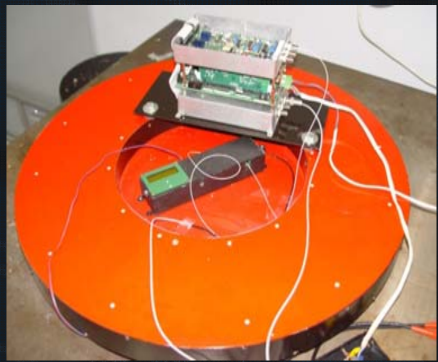

**AFORS-3**

**$\Omega_t$=1.83·10$^{-9}$ rad/s/Hz$^{1/2}$**

L= 14 360 [m], 47 layers, double quadropole winded, $\alpha$ =0.379 [dB/km], loop R=0.315 [m] contains permaloy particles, $\sigma$ = 11.74 [dB], cascade polarizers (46 and 55 [dB]), depolarizer with 0.02 [dB] extinction ratio, $\Delta\lambda$=51,2 [nm], $\lambda$=1311.2 [nm], $P_L$ =17.3 [mW], fg=7.1 kHz.

# AFORSs calibration

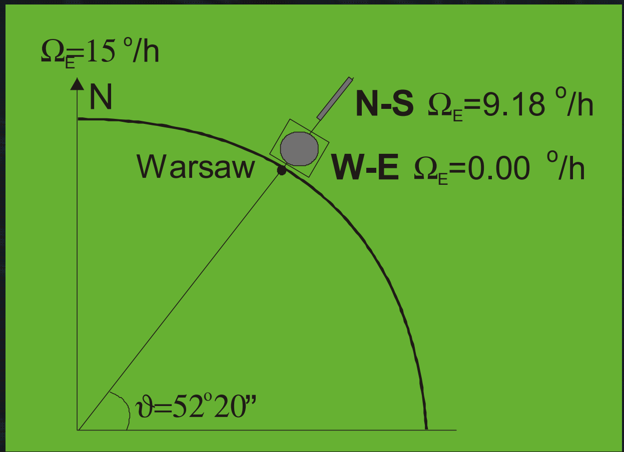


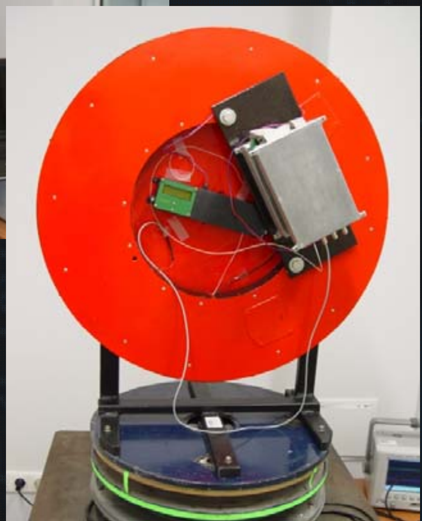

$$\Omega = S_o \arctan\left[S_e \cdot u(t)\right]$$

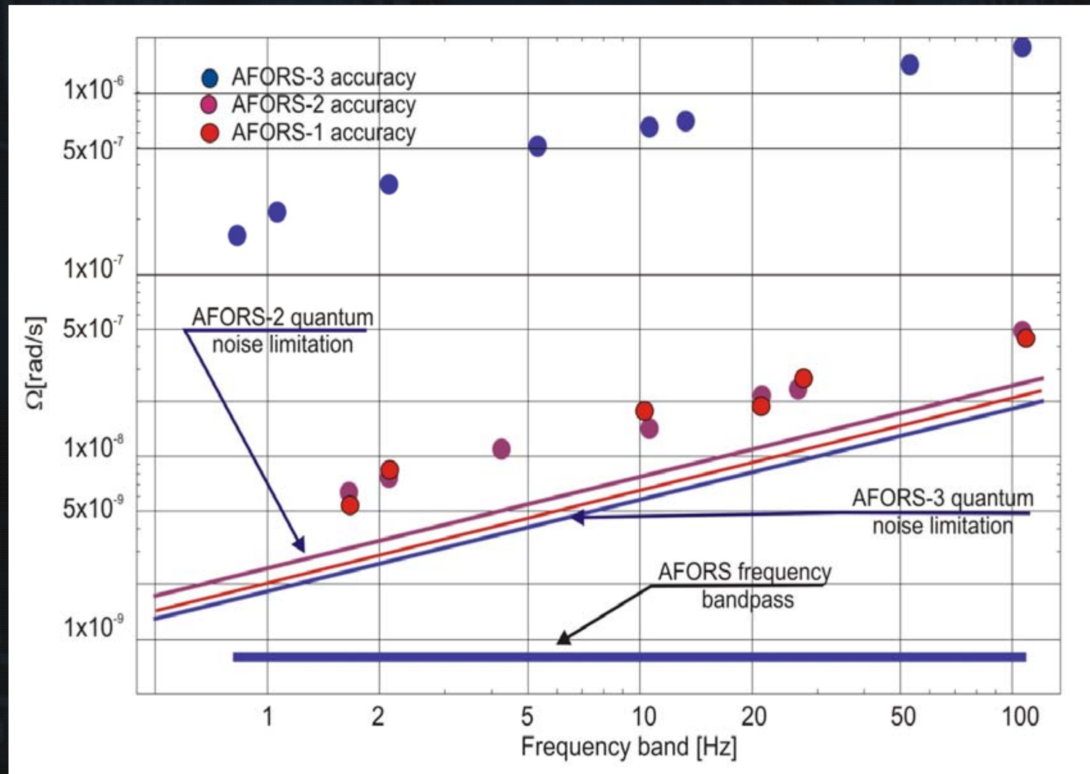


Accuracy

| | | | |
|---|---|---|---|
| ΔB= | 0.83 [Hz] | 13.3 [Hz] | 106.15 [Hz] |
| AFORS-2 | $4.8\ 10^{-9}$ [rad/s] | $1.5\ 10^{-8}$ [rad/s] | $6.1\ 10^{-8}$ [rad/s] |
| AFORS-3 | $1.6\ 10^{-7}$ [rad/s] | $6.9\ 10^{-7}$ [rad/s] | $1.8\ 10^{-6}$ [rad/s] |

# Remote Control


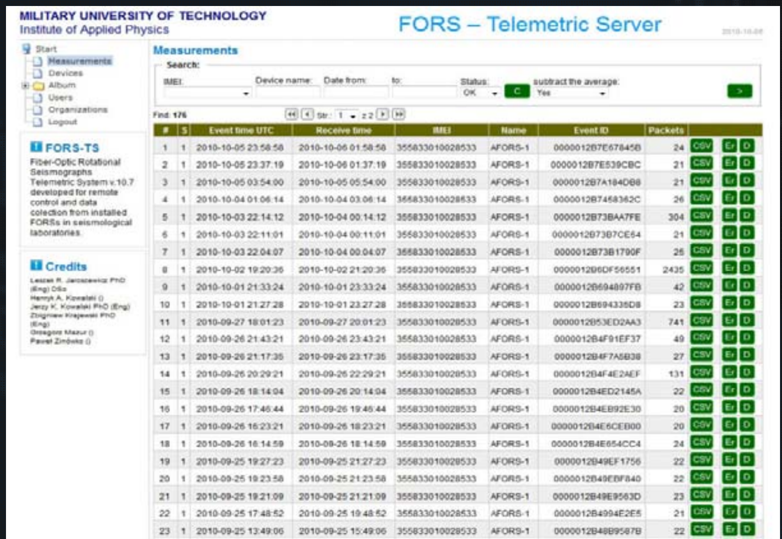


**See POSTER http://fors.m2s.pl**

**Login&password: AFORSbook**


# Example of events recording in Książ


1. Jaroszewicz, L. R., Krajewski, Z.& Solarz, L. (2006). Absolute Rotation Measurement Based on the Sagnac Effect. in: *Earthquake Source Asymmetry, Structural Media and Rotation Effects,* R. Teis-seyre, M. Takeo & E. Majewski E. (Eds), pp.413-438, ISBN 3-540-31336-2, Springer, Berlin
2. Jaroszewicz, L. R. & Krajewski Z. (2008). Application of the Fibre-Optic Rotational Seismometer in Investigation of the Seismic Rotational Waves, *Opto-Electron. Rev.,* Vol.16, No.3, (September 2008), pp. 314-320, ISSN 1230-3402
3. Jaroszewicz, L. R. & Wiszniowski J. (2008). Measurement of Short-Period Weak Rotation Signals, in: *Physics of Asymmetric Continuum: Extreme and Fracture Processes*, R. Teisseyre, H. Nagahama & E. Majewski, (Eds.), pp.17-47, ISBN 978-3-540-68354-4, Springer, Berlin
4. Jaroszewicz, L. R., Krajewski, Z., Kowalski, H., Mazur, G., Zinówko, P. & Kowalski, J. K. (2011a). AFORS Autonomous Fibre-Optic Rotational Seismograph: Design and Application. *Acta Geophys., Vol.* 59, No.3, (March 2011), pp. 578-596, ISSN 0001-5725
5. Jaroszewicz, L. R., Krajewski, Z. & Teisseyre, K. P. (2011b). Usefulness of AFORS – Autonomous Fibre-Optic Rotational Seismograph for Investigation of Rotational Phenomena, *Journal of Seismology,* Special issue: Rotational Ground Motions, 16(4) (2012), 573-586, DOI: 10.1007/s10950-011-9258-3,
6. *L.R. Jaroszewicz, Z. Krajewski, K. P. Teisseyre „Fibre-Optic Sagnac Interferometer as Seismograph for Direct Monitoring of Rotation Events" in D'Amico Sebastiano (Ed): Earthquake Research and Analysis/Book 5, InTech* Open Access Publisher, Rijeka 2012, Ch.16, 335-354, ISBN 9790953-307-681-1

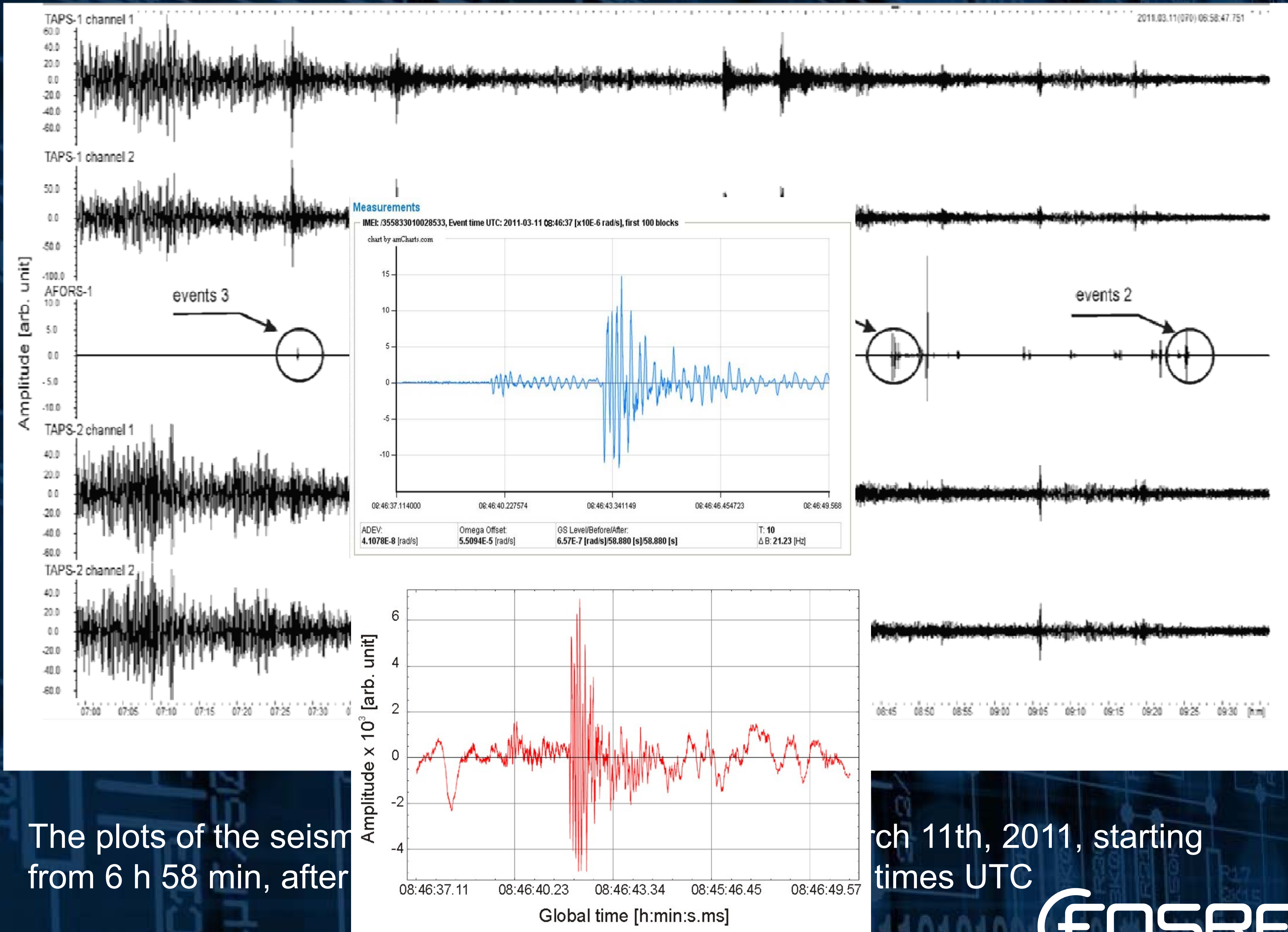


The plots of the seism ... rch 11th, 2011, starting
from 6 h 58 min, after ... times UTC

# Example of events recording in Warsaw

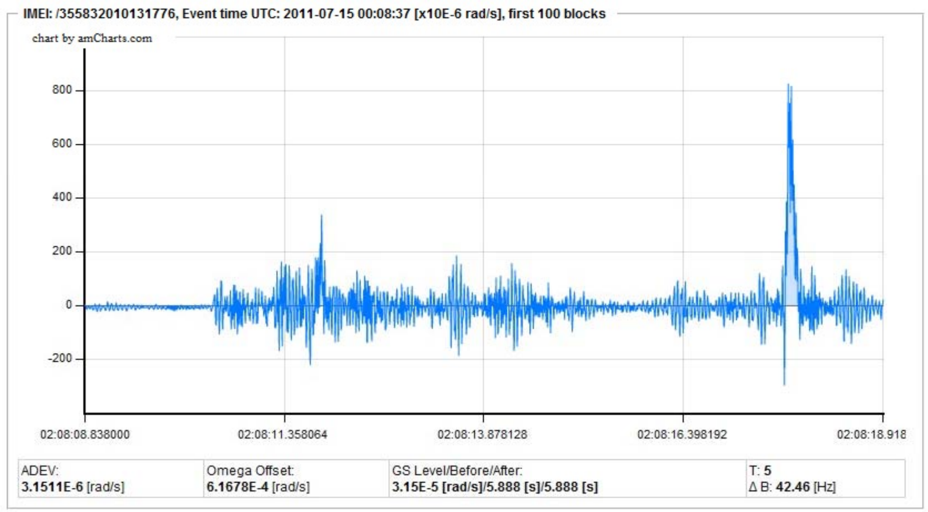


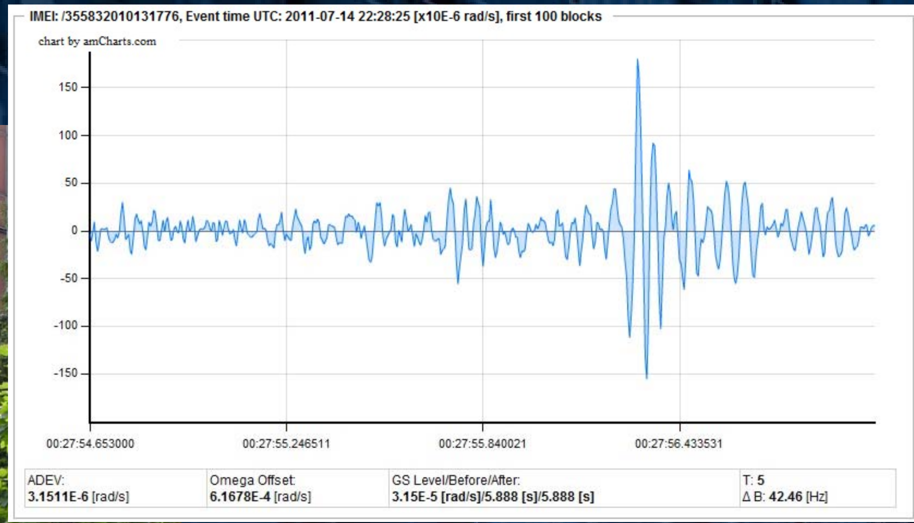


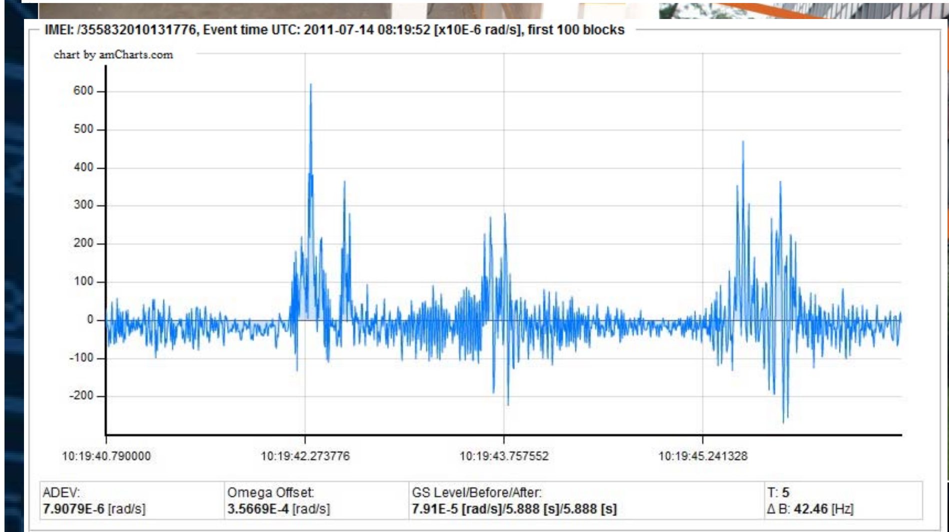


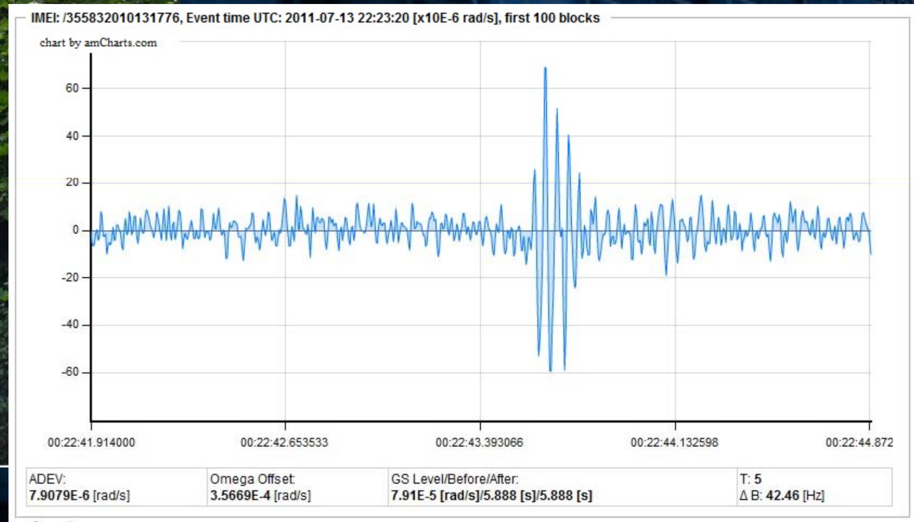


**The data recorded as response for ground moves generated by morning intensity on the street in a distance about 50 m from and parallel to the long building wall.**

**The data recorded as response for ground moves after tram pass through street in distance about 50 m from and parallel to long building wall.**

[L.R. Jaroszewicz, et al., in Oren Lavan, Mario De Stefano (Eds): Seismic Behaviour and Design of Irregular and Complex Civil Structures, Springer 2013, Ch.23, 339-351]

FOSREM

# AFORSs application for monitoring building rotation

AFORS - 2

AFORS - 3

# Outcome

Analogue to digital conversion errors

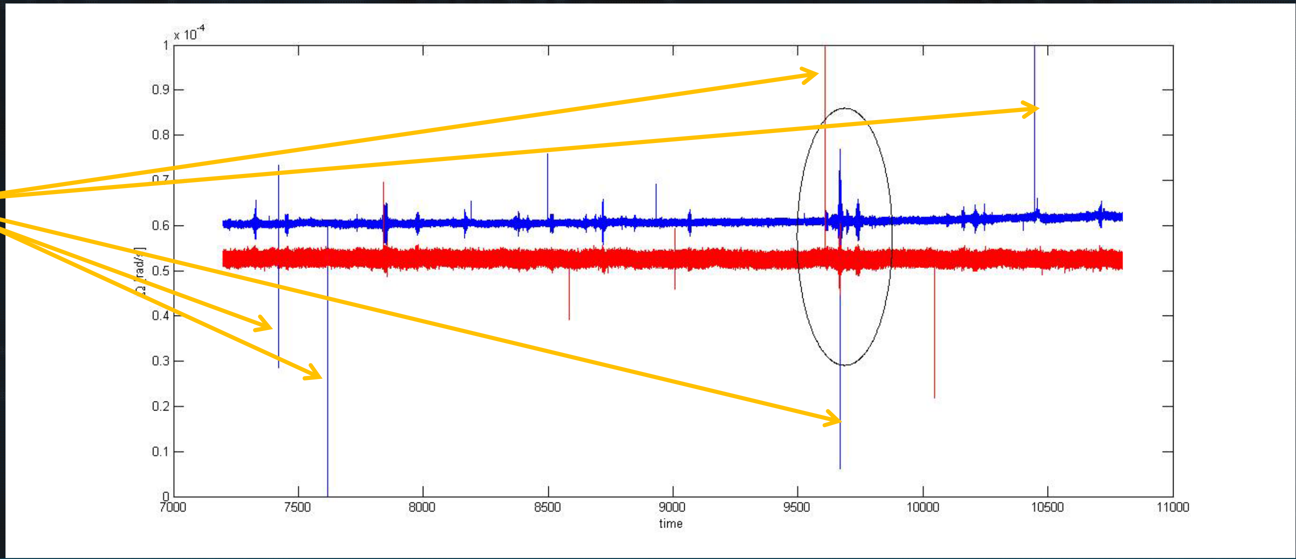


Data after linear regresion aproximation

**AFORS - 2**

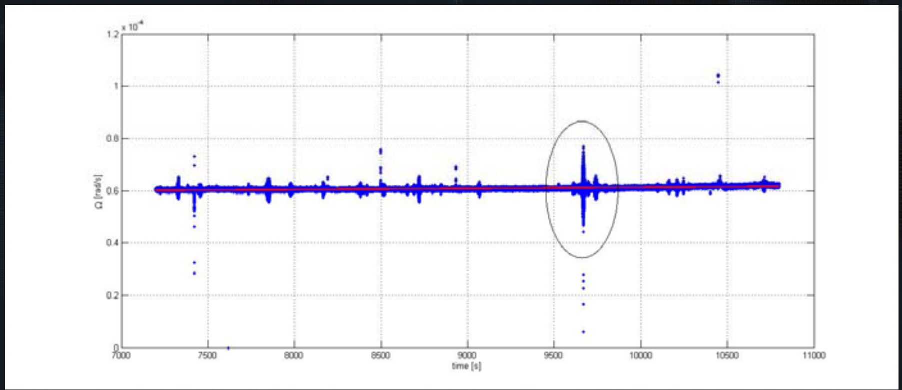

Data after linear regresion aproximation

**AFORS - 3**

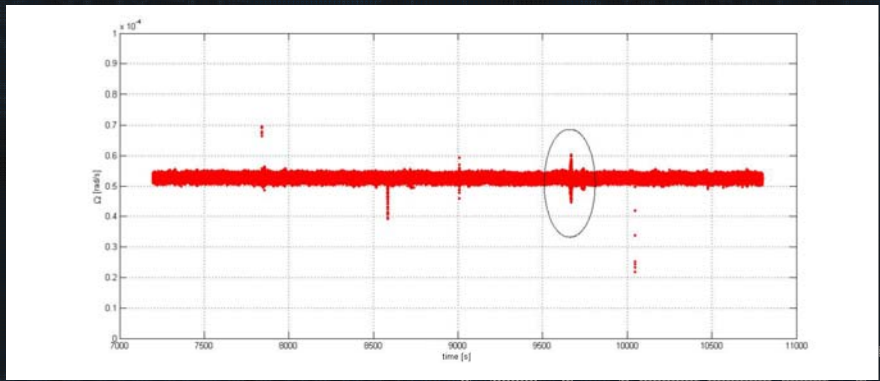

## AFORS – 2, ground floor refernce

## AFORS – 3, ground floor refernce

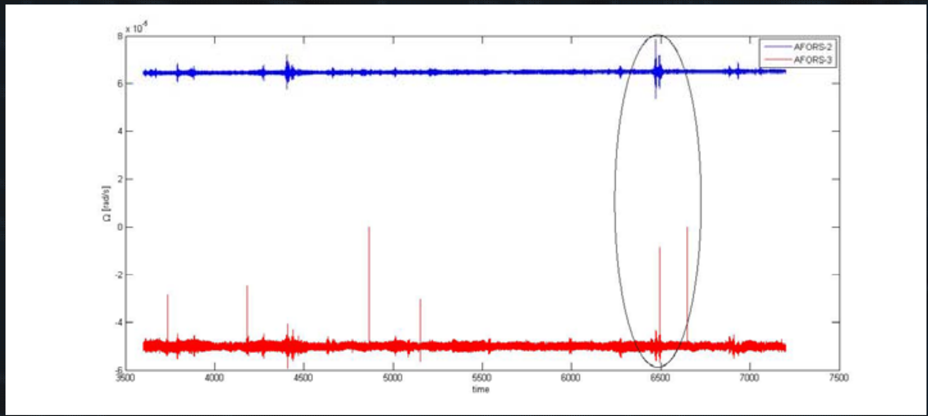


AFORS–2 -- ground floor AFORS–3 -- first floor

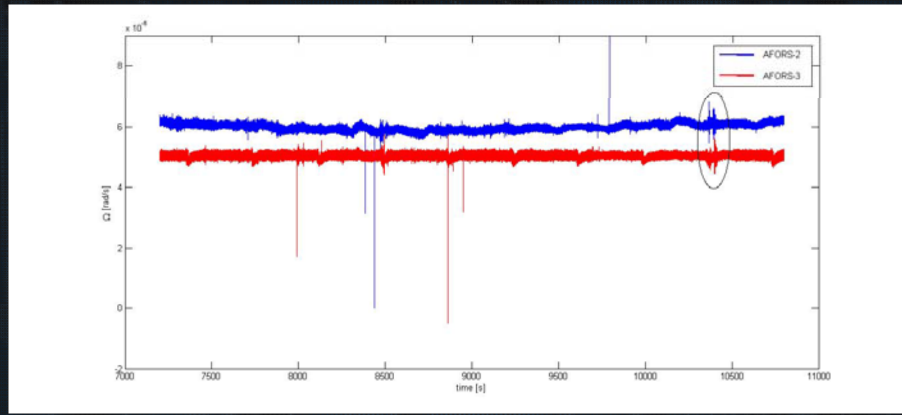


AFORS–3 -- ground floor AFORS–2 -- first floor

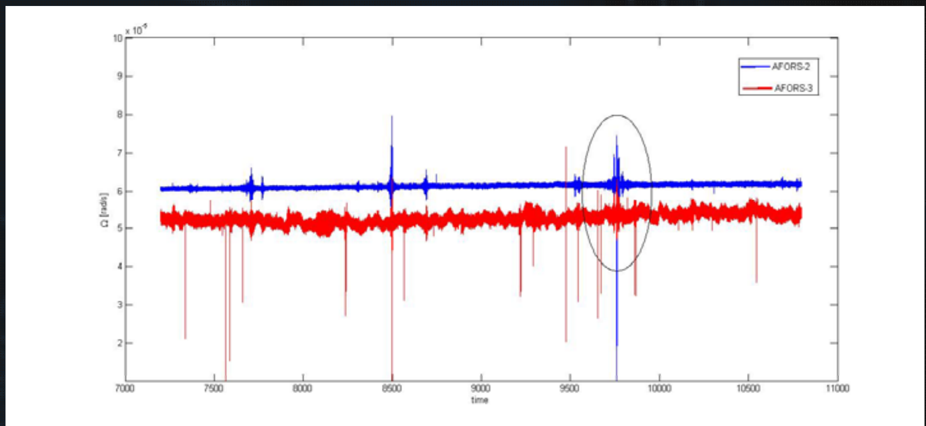


AFORS–2 -- ground floor AFORS–3 -- third floor

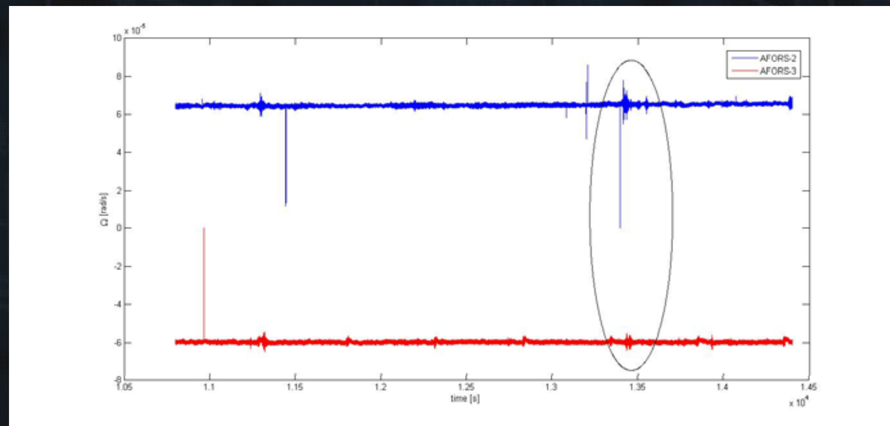


AFORS–3 -- ground floor AFORS–2 -- third floor

| | LOCATION | AMPLITUDE FOR 21 Hz DETECTION BAND [rad/s] | AFTER CALIBRATION [rad/s] |
|---|---|---|---|
| | | | |
| **AFORS-2** | Ground floor | $1{,}586 \cdot 10^{-5}$ | $1{,}586 \cdot 10^{-5}$ |
| **AFORS-3** | Ground floor | $0{,}784 \cdot 10^{-5}$ | $1{,}586 \cdot 10^{-5}$ |
| | | | |
| **AFORS-2** | Ground floor | $0{,}921 \cdot 10^{-5}$ | $0{,}921 \cdot 10^{-5}$ |
| **AFORS-3** | First floor | $0{,}386 \cdot 10^{-5}$ | $0{,}781 \cdot 10^{-5}$ |
| | | | |
| **AFORS-2** | Ground floor | $0{,}942 \cdot 10^{-5}$ | $0{,}942 \cdot 10^{-5}$ |
| **AFORS-3** | Second floor | $0{,}633 \cdot 10^{-5}$ | $1{,}281 \cdot 10^{-5}$ |
| | | | |
| **AFORS-2** | Ground floor | $1{,}855 \cdot 10^{-5}$ | $1{,}855 \cdot 10^{-5}$ |
| **AFORS-3** | Third floor | $1{,}139 \cdot 10^{-5}$ | $2{,}304 \cdot 10^{-5}$ |

| | LOCATION | AMPLITUDE FOR 21 Hz DETECTION BAND [rad/s] | AFTER CALIBRATION [rad/s] |
|---|---|---|---|
| | | | |
| **AFORS-2** | Ground floor | $1{,}586 \cdot 10^{-5}$ | $1{,}586 \cdot 10^{-5}$ |
| **AFORS-3** | Ground floor | $0{,}784 \cdot 10^{-5}$ | $1{,}586 \cdot 10^{-5}$ |
| | | | |
| **AFORS-2** | First floor | $0{,}706 \cdot 10^{-5}$ | $0{,}706 \cdot 10^{-5}$ |
| **AFORS-3** | Ground floor | $0{,}594 \cdot 10^{-5}$ | $1{,}202 \cdot 10^{-5}$ |
| | | | |
| **AFORS-2** | Second floor | $0{,}664 \cdot 10^{-5}$ | $0{,}664 \cdot 10^{-5}$ |
| **AFORS-3** | Ground floor | $0{,}536 \cdot 10^{-5}$ | $1{,}084 \cdot 10^{-5}$ |
| | | | |
| **AFORS-2** | Third floor | $1{,}274 \cdot 10^{-5}$ | $1{,}274 \cdot 10^{-5}$ |
| **AFORS-3** | Ground floor | $0{,}430 \cdot 10^{-5}$ | $0{,}870 \cdot 10^{-5}$ |

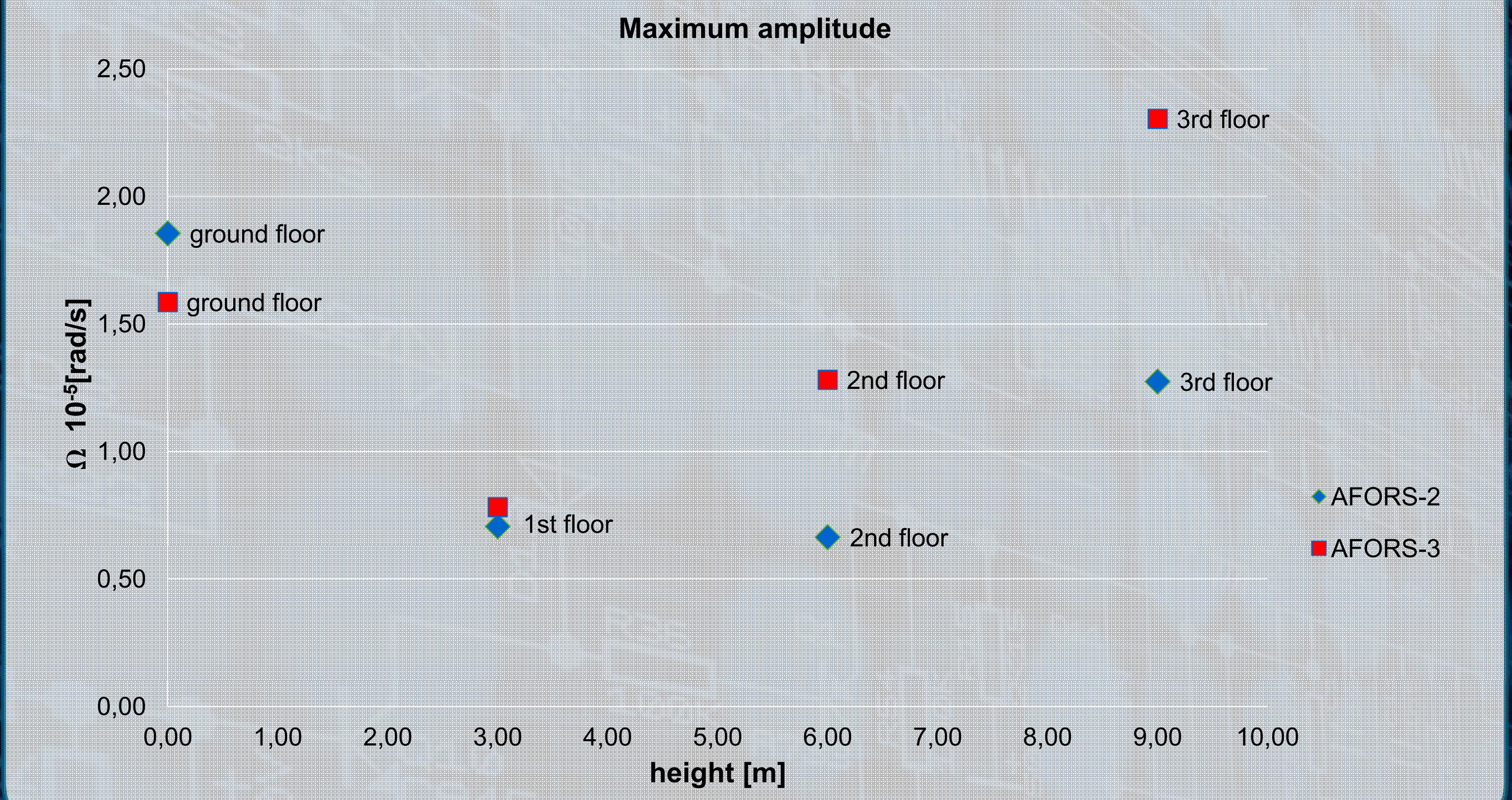

Maximum amplitude
2,50
2,00
1,50
1,00
0,50
0,00
Ω 10-5[rad/s]
ground floor
ground floor
1st floor
2nd floor
2nd floor
3rd floor
3rd floor
AFORS-2
AFORS-3
0,00
1,00
2,00
3,00
4,00
5,00
6,00
7,00
8,00
9,00
10,00
height [m]

# Conclusions

1. The main advantages of AFORS systems:
   - mobile  with remote control of their main parameters,
   - continously monitornig of seismic rotational events,
   - immediate information about recorded events,
   - enough accuracy and frequency bandpass for seismic application.
2. The main disadvantageus of AFORS systems:
   - extremly high cost (uses only for limited applications),
   - problem with verification of their proper works,
   - single axis rotation measurements.
   - errors under highly temperatures (above 60 ºC)
3. Solution FOSREM project – we should have five systems in next year

FOSREM